Magnetic studies of some orthovanadates

Hoan C. Nguyen and John B. Goodenough
Center for Materials Science and Engineering, ETC 9.102, The University of Texas at Austin, Austin, Texas 78712-1063
(Received 7 November 1994; revised manuscript received 22 December 1994)

The perovskites LVO_3 (L=La, Lu, or Y) are canted-spin antiferromagnets. Magnetic susceptibility measurements made on cooling from room temperature in a field of 1 kOe or on heating after cooling in 1 kOe give rise to a sample magnetization **M** that is oriented in opposition to the magnetizing field below 138 K in $LaVO_3$, but in the direction of the magnetizing field in $LuVO_3$ and YVO_3. Orientation of the **M** in $LaVO_3$ in opposition to the magnetizing field **H** occurs on cooling through a first-order magnetostrictive transition at 138 K $< T_N \approx 142$ K that enhances the V^{3+} ion orbital angular momentum. In YVO_3, a first-order magnetic-order phase change at 78 K $< T_N \approx 114$ K shows no evidence of a discontinuous change in the V^{3+} ion orbital angular momentum. The same is true for a phase change in $LuVO_3$ at 83 K $< T_N \approx 105$ K that leaves the magnetic order unchanged. A high-pressure ($P \geq 8$ kbar) $LaVO_3$ phase metastable below 250 °C is antiferromagnetic without spin canting. The "anomalous diamagnetism" previously reported for field-cooled $LaVO_3$ is interpreted to reflect the first observation of a change in the direction of the persistent currents at an ion associated with a discontinuous change in an unquenched orbital angular momentum contribution to the atomic moment; a spin-orbit coupling stronger than the Zeemann coupling of the spin to the magnetizing field reverses the entire atomic moment $\mu_J = g\mathbf{J}\mu_B$. Substitution of La by Lu or Y applies a chemical pressure that suppresses the first-order magnetostrictive distortion responsible for the anomalous diamagnetism.

I. INTRODUCTION

At room temperature, the perovskites LVO_3 are all distorted from cubic to orthorhombic *Pbnm* symmetry by a cooperative rotation of the VO_6 octahedra about $[\bar{1}10]$ axes of the ideal cubic unit cell.[1] This distortion is induced by a mismatch between the equilibrium bond lengths L-O and V-O, where L is a lanthanide atom or Y. A measure of the bond-length mismatch is the tolerance factor

$$t = (L\text{-O})/\sqrt{2}(\text{V-O}) , \quad (1)$$

where the equilibrium bond lengths L-O and V-O may be obtained at room temperature from the table of empirical ionic radii.[2] A $t < 1$ at room temperature for $LaVO_3$ decreases with decreasing ionic radius of the L^{3+} ion; it also decreases with decreasing temperature because of the larger thermal expansion of the L-O bond lengths. A $t < 1$ places the V-O bonds of a cubic structure under compression, the L-O bonds under tension. The cooperative rotation of the VO_6 octahedra buckles the V-O-V bond angles from 180°, thereby relieving the compressive stress on the V-O bonds; it also reduces half of the L-O bond lengths, which relieves the tensile stress on the L-O bonds. If the VO_6 octahedra remain undistorted, the cooperative distortions result in an orthorhombic *Pbnm* structure in which the relation $a \leq b < c/\sqrt{2}$ is normally found.

This O-orthorhombic structure has been differentiated[1] from an O'-orthorhombic structure of the same *Pbnm* symmetry in which a $c/\sqrt{2} < b \leq a$ occurs; a $c/\sqrt{2} < b \leq a$ may be encountered where a cooperative deformation of the VO_6 octahedra is superimposed on a distortion from cubic to orthorhombic symmetry arising from the cooperative rotations of the VO_6 octahedra. At room temperature, both O- and O'-orthorhombic *Pbnm* structures are found among the LVO_3 perovskites; but at 300 K, LVO_3 is paramagnetic and the small difference between O and O' structures appears to reflect only a systematic change of the crystal parameters with the size of the L^{3+} ions.

The deformation of an individual VO_6 octahedron removes an orbital degeneracy associated with a localized $t_2^2e^0$ configuration at an octahedral-site V^{3+} ion. In an octahedral interstice, the $^3F_2$ ground state of a free V^{3+} ion is transformed to a $^3T_{1g}$:$t_2^2e^0$ configuration having a threefold orbital degeneracy. The cubic crystalline fields do not quench totally the orbital angular momentum; the orbitally threefold-degenerate manifold of t orbitals retains azimuthal quantum numbers $m_l = 0, \pm 1$ associated with xy and $yz \pm izx$ constituents referred to a tetragonal deformation or the a_1 and $e_\pm$ constituents referred to a rhombohedral deformation of an elementary VO_6 octahedron. The preferred symmetry of the Jahn-Teller deformation of a VO_6 octahedron is rhombohedral. However, the sign of the deformation, i.e., $\alpha > 60°$ vs $\alpha < 60°$, depends upon whether the Jahn-Teller deformation that removes the degeneracy quenches or enhances the orbital angular momentum.

In order to determine the sign of the deformation δ to be stabilized, it is necessary to consider three terms in the same order of perturbation theory: the noncubic component

$$V_{NC} = \delta(L_z^2 - \tfrac{2}{3}) \quad (2)$$

of the crystal-field splitting, the spin-orbit coupling

$$V_{LS}=\lambda \mathbf{L}\cdot\mathbf{S}\ , \tag{3}$$

and the Zeemann energy H_z arising from the internal molecular magnetic field $\mathbf{H}_i$ at a local magnetic moment $\mu_J=g\mathbf{J}\mu_B$ below a long-range magnetic-ordering temperature, where the spectroscopic splitting factor g is a tensor defined by the relation

$$\mu_B\mathbf{H}_i\cdot g\cdot\mathbf{S}'=\langle\psi_g|H_z|\psi_g\rangle \tag{4}$$

and the Zeeman energy is

$$H_Z=\mu_B\mathbf{H}_i\cdot(ak_c\mathbf{L}+2\mathbf{S})\ . \tag{5}$$

For a $^3T_{1g}$ configuration, the parameter a that transforms the orbitally threefold-degenerate t manifold to the equivalence of a p manifold is $a=-\frac{3}{2}$;[3] the fraction $k_c\approx 0.8-0.9$ reflects the reduction in the spin-orbit coupling parameter λ resulting from covalent mixing with the oxygen near neighbors.

Most threefold-degenerate t-orbital configurations are unbiased with respect to the sign of δ to second order in δ/λ as long as there is no long-range magnetic order ($\mathbf{H}_i=0$). However, long-range magnetic order ($\mathbf{H}_i\neq 0$) introduces an anisotropic Zeemann energy ($g_\parallel\neq g_\perp$ to the unique axis) that stabilizes a $\delta<0$ with spins parallel to the unique local axis to first order in δ/λ.[4] This situation means that a cooperative Jahn-Teller deformation occurring above a long-range magnetic ordering temperature, i.e., where $\mathbf{H}_i=0$, generally has a sign that quenches the orbital angular momentum as illustrated in Fig. 1(a); those that occur at or below a magnetic-ordering temperature have a sign that preserves the orbital angular momentum, Fig. 1(b). In the latter case, long-range ordering of the spins introduces a long-range ordering of the orbital angular momenta through the spin-orbit coupling, which in turn induces a cooperative deformation that preserves the orbital angular momentum at an individual Jahn-Teller ion. Moreover, the coupling of the μ_J to the deformation gives rise to a giant *magnetostriction and single-ion magnetocrystalline* anisotropy.

The $^3T_{1g}$ configuration at an octahedral site V^{3+} ion differs in only one respect; it is biased already to $|\delta/\lambda|^2$ in favor of a local deformation that preserves the orbital angular momentum where $\mathbf{H}_i=0$. However, disordering of the spins in the paramagnetic temperature range must suppress, by spin-orbit coupling, any cooperative crystallographic distortion that would conserve the orbital angular momentum.

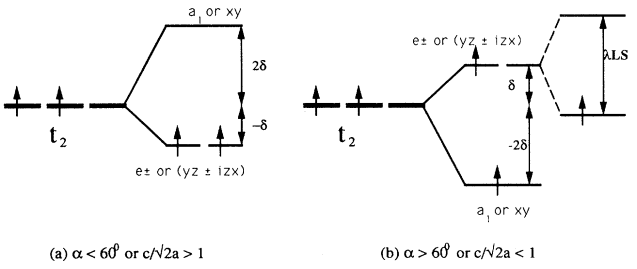

FIG. 1. Splitting of the t_2^2 configuration in the noncubic crystal field: (a) rhombohedral with $\alpha<60°$ or tetragonal with $c/\sqrt{2}a>1$ quenches the orbital and angular momentum, (b) rhombohedral with $\alpha>60°$ or tetragonal with $c/\sqrt{2}a<1$ preserves the orbital angular momentum.

The present study was originally initiated within the context of an exploration of the $La_{1-x}Ca_xVO_3$ system, which exhibits a transition from antiferromagnetic insulator to Pauli-paramagnetic metal or itinerant-electron antiferromagnet (depending on oxygen content) on proceeding from $x=0$ to $x=1$.[5] In the course of this study, two independent reports[6,7] of a giant diamagnetism in $LaVO_3$ confirmed our preliminary data. Giant diamagnetism was found if the susceptibility was measured in a magnetizing field $\mathbf{H}<1$ kOe on heating after first cooling in the measuring field from room temperature to liquid-He temperature. It was not found if the sample was first cooled in zero applied field.

We have reported elsewhere[8] experiments that demonstrate the origin of the apparent diamagnetism in $LaVO_3$ is a canted-spin ferromagnetism that orients its magnetization *in opposition* to the *magnetizing field* on cooling in the field through a magnetostrictive crystallographic transition temperature $T_t<T_N$. The individual μ_V respond normally to the magnetizing field below T_t; it is the direction of the spin canting that is anomalous in lower applied fields. A recent structural refinement as a function of temperature[9] has shown a cooperative distortion to monoclinic $P2_1/a$ symmetry below T_t in which each octahedron opens two opposite faces to introduce a rhombohedral ($\alpha>60°$) component to the local crystalline field, and an unpublished 4-K magnetic structure[10] that was kindly supplied to us by M. Marezio shows a canted-spin configuration below T_t with vanadium magnetic moments oriented nearly parallel to the rhombohedral axes.

We compare here the magnetometer data for $LaVO_3$ with those for two related perovskites, YVO_3 and $LuVO_3$, which differ significantly from those for $LaVO_3$. In each of these three perovskites, the L^{3+} ion carries no magnetic moment, and the differences in their magnetic properties appear to be due only to differences in the size and basicity of the L^{3+} ions. These differences modulate both the strength of the V-O-V interactions and the V-O-V bond angles. We argue that the data reflect a first-order phase change between a localized-electron and an itinerant-electron antiferromagnetism. A cooperative Jahn-Teller distortion is associated only with the former, and it introduces at the transition temperature T_t a discontinuous change in the orbital angular momentum that reverses the persistent atomic current responsible for the orbital angular momentum. Spin-orbit coupling then inverts the spins as well to cause a reversal in direction of the total vanadium moment on traversing T_t.

II. EXPERIMENTAL DETAILS

The perovskites LVO_3 were obtained by reducing LVO_4 powder in flowing hydrogen at 1100 °C with several intermittent grindings. The LVO_4 powders with $L=$ La, Y, or Lu were prepared by standard solid-state

reaction in air at 850 °C of stoichiometric mixtures of dried L_2O_3 and V_2O_5 powders. Once a single-phase perovskite had been obtained, the compound was sintered in ultrapure argon at 1400 °C.

All samples LVO_3 and $La_{1-x}Y_xVO_3$ were single-phase to powder x-ray diffraction taken with a Philips diffractometer and Cu $K\alpha$ radiation. The peak positions were calibrated against Si as an internal standard, and the lattice parameters were obtained with a least-squares fitting procedure.

The oxygen content of the LVO_3 powders was determined with a Perkin-Elmer TGA-7 thermogrametric analyzer (TGA) from the weight gain on heating in air to 700 °C to oxidize the vanadium to V^{5+}.

Magnetic-susceptibly, $\chi = M/H$, measurements were obtained from 5 to 300 K with a superconducting quantum interference device (SQUID) magnetometer in magnetic field strengths $0 \leq \mathbf{H} \leq 50$ kOe.

III. RESULTS

A. Structures

Room-temperature powder x-ray-diffraction data showed all the LVO_3 perovskites were orthorhombic, space group *Pbnm*, isostructural with $GdFeO_3$. The lattice parameters and unit-cell volumes are listed in Table I for L = La, Y, and Lu; they show a decrease in unit-cell volume and an increase in the ratio $c/\sqrt{2}a$ with decreasing size of the L^{3+} ion. In all samples, an oxygen stoichiometry 3.00 ± 0.02 was determined from TGA measurements.

Zubkov, Bazuev, and Shveikin,[11] Dougier and Hagenmuller,[12] and Bordet *et al.*[9] have reported an anomalous drop in the ratio $c/\sqrt{2}a$ of $LaVO_3$ on cooling in zero field below $T_t < T_N$, which is indicative of a Jahn-Teller distortion that enhances the orbital angular momentum in the magnetically ordered state. We shall refer to this transition as a magnetostrictive distortion. Borukhovich, Bazuev, and Shveikin[13,14] have reported two λ-type specific-heat anomalies near 140 K separated by only 2–3 K; the lower one corresponds to the magnetostrictive distortion setting in below a $T_t < T_N$ and the upper one to a Néel temperature T_N. In contrast, the $c/\sqrt{2}a$ ratio of YVO_3 and $LuVO_3$ remains $c/\sqrt{2}a > 1$ down to 77 K and shows no anomalous variation near T_N.[11] However, YVO_3 has a $b < a < c/\sqrt{2}$ at $T_s \approx 77$ K where the spin configuration changes and below which the volume and the ratios b/a and $c/\sqrt{2}a$ are reduced.[15]

B. Magnetic data for $LaVO_3$

In order to understand the origin of the anomalous diamagnetism reported independently by Shirakawa and Ishikawa[6] and Mahajan *et al.*[7] for $LaVO_3$ if cooled in a magnetic field $\mathbf{H} \leq 1$ kOe, we performed several experiments.[8]

Figure 2 shows the temperature dependence of the molar susceptibility χ_m obtained on heating in an applied field $\mathbf{H} = 1$ kOe after cooling in zero magnetic field [zero-field-cooled (ZFC) case] and after cooling to 4 K from room temperature at $\mathbf{H} = 1$ kOe (1-kOe case). A sample sintered at 1100 °C gave the same qualitative behavior as a sample sintered at 1400 °C. The data are similar to those reported in the literature.[6,7] Quenching into liquid He from room temperature in zero magnetic field [zero-field-quenched (ZFQ) case] or in a field of 1 kOe (FQ 1-kOe case) gave curves similar, respectively, to the ZFC and FC 1-kOe cases shown in Fig. 2.

The ZFC (and ZFQ) curves show a Néel temperature $T_N \approx 142$ K typical of an antiferromagnet. Any weak ferromagnetism due to spin canting is not apparent not only because of a random orientation of the magnetic domains in the ZFC sample, but also because the magnetostrictive distortion below T_t can be expected to lock the randomly oriented domains to local lattice deformations so that only reversible magnetic phenomena are found at 1 kOe. On the other hand, the FC 1-kOe (or FQ 1-kOe) curves show an abrupt transition at a $T_t \approx 138$ K below which χ_m drops sharply with decreasing temperature from positive to negative values. The onset of the magnetic transition at T_t in the FC 1-kOe curves may be taken to mark the onset of the magnetostrictive distortion made evident by the drop in $c/\sqrt{2}a$ ratio below T_t. Moreover, the higher value of the FC χ_m in the internal $T_t < T < T_N$ compared to that of the ZFC χ_m in the same temperature interval suggests the presence of a canted-spin ferromagnetism appearing below T_N as a result of the Dzialoshinskii antisymmetric exchange. In fact, neutron-diffraction measurements[10–12] have verified the presence of a ferromagnetic component to the spin configuration below T_t. This finding and the drop to negative values of the FC χ_m curve below T_t indicates that below T_t the ferromagnetic component of the canted-spin configuration becomes oriented in opposition to the magnetizing field on cooling the samples through T_t in 1 kOe. The "anomalous diamagnetism" previously reported is only a manifestation of this deeper anomaly.

The x-ray data of Bordet *et al.*[9] show that the sharp

TABLE I. Room-temperature lattice parameters of LVO_3.

Sample	a (Å)	b (Å)	c (Å)	$c/\sqrt{2}a$	V (Å)^3	Phase
$LaVO_3$	5.547	5.546	7.842	0.99	241.23	O'
YVO_3	5.273	5.592	7.564	1.01	223.02	O
$LuVO_3$	5.209	5.564	7.531	1.02	218.29	O

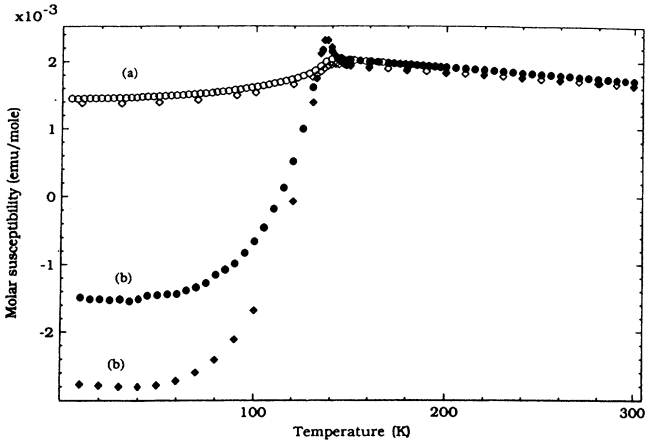

FIG. 2. Molar susceptibility vs temperature curves of $LaVO_3$ measured in 1 kOe after (a) ZFC and (b) FC at 1 kOe from room temperature to 5 K for a sample sintered at 1100 °C (circles) and 1400 °C (diamonds).

decrease in the $c/\sqrt{2}a$ ratio on cooling through T_t is associated with an orthorhombic-to-monoclinic, space group $P2_1/a$, transition. An expansion of opposite faces of each elementary VO_6 octahedron occurs below T_t, which is consistent with a stabilization of the a_1 orbital relative to the two $e_\pm$ orbitals in an orthorhombic component of the VO_6 deformation as illustrated in Fig. 1(b). Moreover, the magnetic order determined from neutron data[10] has individual vanadium moments $1<\mu_V<2\mu_B$ oriented nearly parallel to one of the $\langle 111 \rangle$ axes of its elementary octahedron. The data therefore indicate that a magnetostrictive distortion of VO_6 occurs below T_t to give an important rhombohedral ($\alpha > 60°$) component to the deformation of the individual VO_6 octahedra. Such a deformation implies the existence of a giant magnetocrystalline anisotropy that holds the individual μ_V to an orientation nearly parallel to one of the $\langle 111 \rangle$ axes of an elementary VO_6 octahedron, thereby inhibiting domain-wall motion and flopping of the spins to a new orientation in a strong magnetic field.

In order to test this deduction, a series of curves of magnetization **M** versus applied magnetic field **H** were taken.[8] All curves showed little hysteresis, which is indicative of almost completely reversible magnetization processes up to an applied field strength $\mathbf{H}=50$ kOe; the magnetocrystalline anisotropy is clearly enormous. In addition, the FC 1-kOe curves are all shifted from the origin to negative **M** values at $\mathbf{H}=0$, i.e., $\Delta\mathbf{M}<0$, consistent with the negative χ_m shown for the FC 1-kOe curves in Fig. 2 as measured in 1 kOe. However, a $d\mathbf{M}/d\mathbf{H}>0$ is not anomalous; the individual spins rotate in the direction of **H** against the constraining anisotropy field. For FC 1-kOe samples, the magnetization **M** at 20 K changes from negative to positive at an $H_{cr}=3$ kOe. The slopes of the FC 1-kOe **M**-**H** curves are a little larger than the ZFC curves and they increase with temperature as expected for a decrease with increasing temperature in the magnitude of the magnetocrystalline anisotropy. Nevertheless, there is little hysteresis in curves cycled to 50 kOe even at 130 K, which is close to the transition temperature $T_t \approx 138$ K. The magnetic data clearly indicate that the transition at T_t is magnetostrictive and gives rise to a giant magnetocrystalline anisotropy for the individual μ_V.

To demonstrate that the apparent anomalous diamagnetism observed in $LaVO_3$ is due to an orientation below T_t of a weak ferromagnetism oriented in opposition to the magnetizing field, we performed the following experiments.[8]

(1) Samples were ZFC to $T_a=150$, 138, and 130 K and FC at 1 kOe from T_a to 4 K before a χ_m vs T heating curve was obtained. We refer to these curves as FC ($T<T_a$). The FC ($T<130$ K) curve was similar to the FC 1-kOe curves, the FC ($T<150$ K) curve was similar to the ZFC curves, and the FC ($T<138$ K) had an intermediate character; $T_a \approx T_t$ gives rise to some regions exhibiting a ZFC behavior and others a FC 1-kOe behavior, which result in two peaks in the $\chi_m(T)$ curve.[8]

(2) We next cooled a sample in kOe to temperatures $T_a=150$, 138, and 130 K and ZFC from T_a to 4 K before a $\chi_m(T)$ curve taken on heating was obtained. We refer to these curves as FC ($T>T_a$). The FC ($T>130$ K) curve was like the ZFC curves, the FC ($T>150$ K) curve was like the FC 1-kOe curves, and the FC ($T>138$ K) curve was intermediate between the two as would be expected for two types of regions coexisting at $T_a=138$ K.[8]

(3) We then cooled a sample in 1 kOe to 80 K in a vibrating-sample magnetometer and rotated the sample about an axis perpendicular to the field direction. As can be seen in Fig. 3 of Ref. 8, the magnetization **M** changes from negative to positive on rotating 180°; it returns to its original negative (diamagnetic) value on rotating 360°. Moreover, after removal of the applied magnetic field, a remanant magnetization of the FC 1-kOe sample gave a similar behavior. The remanant magnetization is always smaller than that in an applied field, regardless of orientation of the magnet with respect to the field, because $d\mathbf{M}/d\mathbf{H}>0$; see Fig. 4 of Ref. 8.

(4) Increasing the field strength **H** in which the sample was cooled through T_t increased the negative shift of the nearly linear, nonhysteretic **M** vs **H** curves at 20 K and increased H_{cr} to $H_{cr}=7$ kOe for the FC 50-kOe case; see Fig. 4 of Ref. 8.

C. High-pressure $LaVO_3$

The magnetic data for $LaVO_3$ prepared at atmospheric pressure are in marked contrast with those obtained on samples prepared at 1000 °C under a pressure $P>8$ kbar; see Fig. 3. The FC 1-kOe curve for the high-pressure phase exhibits neither a weak ferromagnetism nor an "anomalous diamagnetism" even though the Néel temperature remains at $T_N \approx 142$ K.

This change in magnetic properties reflects stabilization of a new perovskite phase, metastable at atmospheric pressure and room temperature, which is stabilized under

TABLE II. Room-temperature lattice parameters, paramagnetic Curie temperature, molar Curie constants, Néel temperature, and magnetostrictive temperature T_t of $LaVO_3$ with or without pressure synthesis.

Pressure	a (Å)	b (Å)	c (Å)	V (Å^3)	$c/\sqrt{2}a$	Θ (K)	C_M	T_N (K)	T_t (K)
Ambient	5.547	5.546	7.842	241.2	0.999	−670	1.60	142	134
8 kbar	5.498	5.584	7.810	239.8	1.005	−666	1.52	145	
15 kbar	5.434	5.575	7.794	236.2	1.015	−541	1.41	145	
15 kbar	5.544	5.530	7.832	240.1		after heating to 250 °C in hydrogen			
15 kbar	5.540	5.530	7.849	240.4		after heating to 450 °C in hydrogen			

hydrostatic pressure $P > 8$ kbar. The room-temperature lattice parameters of the ambient-pressure phase are compared in Table II with the lattice parameters of the metastable high-pressure phase prepared at $P = 8$ and 15 kbar. A change in the axial ratio $c/\sqrt{2}a < 1$ to $c/\sqrt{2}a > 1$ signals a change from O′-orthorhombic to O-orthorhombic symmetry in the metastable high-pressure phase with a small volume change $\Delta V \approx -5$ Å^3 indicative of a first-order phase change. Differential scanning calorimetry (DSC) at 10 °C/min indicates that an irreversible first-order phase change from the metastable 15-kbar phase to the ambient-pressure phase occurs below 350 °C, Fig. 4. Heating a 15-kbar metastable sample to 250 °C in flowing hydrogen gave room-temperature lattice parameters similar to those of the parent ambient-pressure phase (Table II), indicating that the metastable 15-kbar phase reverts to the ambient-pressure phase already at 250 °C. Magnetic data confirm that the properties of the ambient-pressure phase are reestablished.

An alternate way to apply pressure on the VO_3 array of the $LaVO_3$ perovskite is to replace La by a smaller L atom; a smaller L atom reduces the tolerance factor $t < 1$ of Eq. (1), which places the VO_3 array under a greater compressive stress as a result of the larger mismatch between the equilibrium $(L\text{-O})/\sqrt{2}$ and V-O bond lengths. We substituted $L = $ Y or Lu so as to avoid complications arising from the presence of an atomic moment on the L^{3+} ions.

Our initial strategy was to prepare the system $La_{1-x}Y_xVO_3$ in order to examine the evolution of properties with increasing pressure on the VO_3 array. However, we encountered a broad two-phase region in the system appearing in the range $0.08 < x < 0.92$; the phase with $0 < x < 0.08$ was O' orthorhombic at room temperature, and the phase with $0.92 < x < 1.0$ was O orthorhombic. This finding is consistent with a first-order transition between the atmospheric-pressure and high-pressure

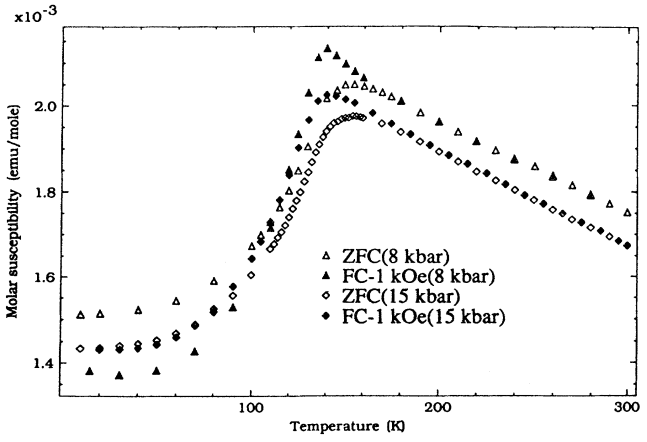

FIG. 3. Molar susceptibility vs temperature of high-pressure $LaVO_3$ prepared at 8 or 15 kbar taken on heating after a ZFC and FC at 1 kOe.

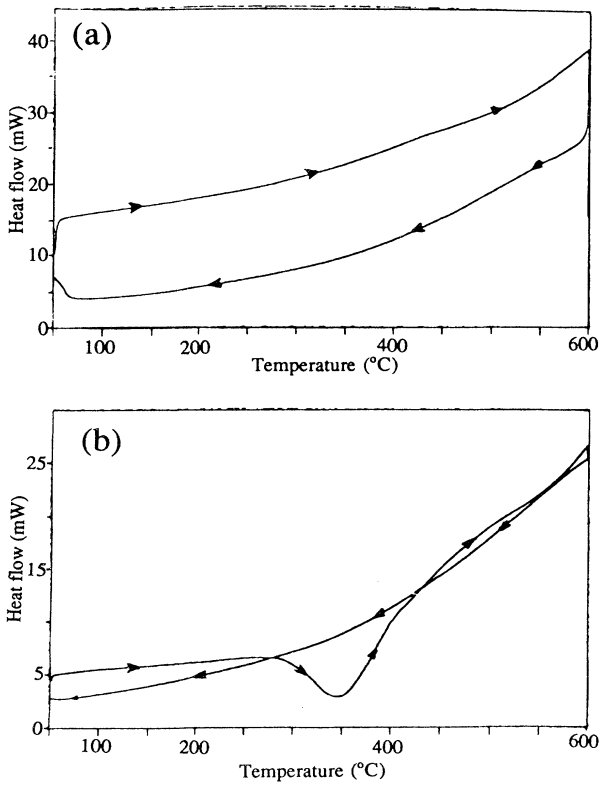

FIG. 4. Differential scanning calorimetry curves of (a) ambient-pressure $LaVO_3$ and (b) 15 kbar $LaVO_3$ taken at 10 °C/min.

phases of $LaVO_3$. We concluded that YVO_3 and $LuVO_3$ should be representative of high-pressure $LaVO_3$.

D. Magnetically ordered spin configurations

Bertaut[16] has adopted the notation of Koehler, Wollan, and Wilkinson[17] to describe the possible antiferromagnetic spin configurations compatible with the *Pbnm* crystallographic space group. Figure 5 represents the V atoms of a pseudotetragonal LVO_3 structure. Linear combinations of the spin components that transform into themselves are chosen as the base vectors of the irreducible representations:

$$\begin{aligned} F&=S_1+S_2+S_3+S_4\ , \\ G&=S_1-S_2+S_3-S_4\ , \\ C&=S_1+S_2-S_3-S_4\ , \\ A&=S_1-S_2-S_3+S_4\ . \end{aligned} \tag{6}$$

Subjecting these vectors to the crystallographic symmetry operations generates the four possible representations of the base vectors shown in Table III. The x,y,z directions are taken parallel to the a,b,c axes of the pseudotetragonal unit cell.

Huang *et al.*[10] have determined the magnetic order of $LaVO_3$ at 100 K to be C_yF_x, which means antiferromagnetic coupling within the c-a basal plane and ferromagnetic coupling along the a axis. The antiferromagnetic component in the c-a plane is oriented along the pseudotetragonal b axis and hence along a [1 1 0] axis of the elementary VO_6 octahedra; the ferromagnetic component makes the net spin approach a [1 1 1] or [$\bar{1}\,\bar{1}$1] axis of an elementary VO_6 octahedron where there is no cooperative tilting of the octahedra responsible for orthorhombic symmetry. The greater the tilt of the octahedra, the greater is the deviation of the spin axis from one of the ⟨111⟩ axes of the elementary octahedra.

TABLE III. Representation of base vectors of vanadium ion with the space group *Pbnm* of orthovandites (after Ref. 16).

Representations	Base vector for vanadium ion		
Γ_1	A_x	G_y	C_z
Γ_2	F_x	C_y	G_z
Γ_3	C_x	F_y	A_z
Γ_4	G_x	A_y	F_z

E. Magnetic data for YVO_3

Zubko, Bazuev, and Shveikin[11] have reported a change in the ordered spin configuration at a $T_s \approx 78$ K from a low-temperature C_yF_x to a G_xF_z arrangement stable below a temperature $T_N \approx 114$ K, which they assumed to be the Néel temperature. Kawano, Yoshizawa, and Ueda[15] confirm a $T_s \approx 77$ K $< T_N \approx 118$ K, but they found a G-type order below T_s and a C-type order above T_s with a first-order phase change occurring at T_s. A vanadium moment $1.2 \leq \mu_V \leq 1.6\mu_B$ was found at 4.2 K. Both groups also reported a $c/\sqrt{2}a > 1$ decreasing linearly with temperature to 78 K with no structural anomaly apparent at T_N. Borukhovich, Bazuev, and Shveikin[18] confirmed specific-heat anomalies at T_s and T_N. Both spin configurations could have a spin axis approaching a [111] axis of an elementary VO_6 octahedron.

In Fig. 6 we show the temperature variation of the molar susceptibility taken on heating from 5 K in 1 kOe (the magnetization is $\mathbf{M}=\chi_m \times 1$ kOe) for two YVO_3 samples, one sintered in argon at 1100 °C and the other at 1400 °C. The ZFC curves show clearly one transition near 114 K,

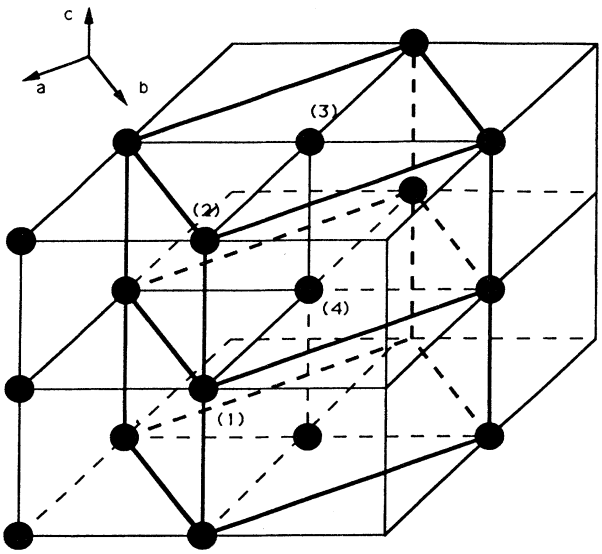

FIG. 5. Labeling vanadium positions in perovskite structure of *Pbnm* symmetry for LVO_3, where L is lanthanide or Y.

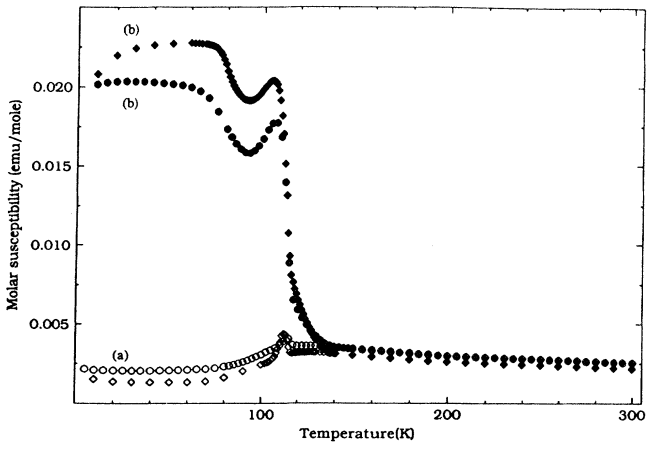

FIG. 6. Molar susceptibility vs temperature curves of YVO_3 measured in 1 kOe after (a) ZFC and (b) FC at 1 kOe from room temperature to 5 K for a sample sintered at 1100 °C (circles) and 1400 °C (diamonds).

no compelling evidence for a transition at $T_s \approx 78$ K, and a small change of slope at about 130 K. The FC 1-kOe curves, on the other hand, show a clear anomaly at $T_s \approx 78$ K, a sharp transition at $T_N \approx 114$ K, and evidence of considerable short-range order between T_N and a short-range-ordering temperature $T_{SO} \approx 130$ K. Unlike $LaVO_3$, the canted-spin ferromagnetism is oriented in the direction of the magnetizing field at all temperatures $T < T_N$; there is no anomalous diamagnetism. Figure 6 indicates a large enhancement of the susceptibility at T_N, a small enhancement at T_s; the enhancement at T_N is unusual and may represent a spin reorientation on passing from short-range to long-range order.

Figure 7 compares $\chi_m(T)$ curves taken on heating in 1 kOe after a FC-1 kOe to 5 K with those for a FC ($T > T_a$) at 1 kOe to $T_a = 100$ or 120 K followed by a ZFC to 5 K. The curve for $T_s < T_a = 100$ K $< T_N$ gave a magnetization $\mathbf{M} = \chi_m \times 1$ kOe identical to that of the same sample, FC-1 kOe to 5 K, but the curve for $T_N < T_a = 120$ K $< T_{SO}$ gave a reduced magnetization. This behavior indicates that the magnetic-domain configuration established on cooling through T_N to 100 K in 1 kOe is similar to that established on cooling through T_s to 5 K in 1 kOe, but cooling through T_{SO} in 1 kOe gives a smaller volume of magnetic domains oriented with a component of the magnetization parallel to **H**. Moreover, the increases in χ_m to a maximum at T_N on heating in 1 kOe suggests an important increase in the susceptibility at a change from long-range to short-range order; a small enhancement of χ_m is found at the spin-configuration change occurring at T_s.

In an attempt to clarify this situation further, a sample of YVO_3 was ZFC to $T_a = 60$, 90, or 120 K and then FC ($T < T_a$) at 1 kOe from T_a to 5 K. The $\chi_m(T)$ curves obtained on subsequent heating in a 1-kOe measuring field are shown in Fig. 8. With $T_a = 60$ K, the $\chi_m(T)$ curve was similar to that for ZFC to 5 K; it was not possible to

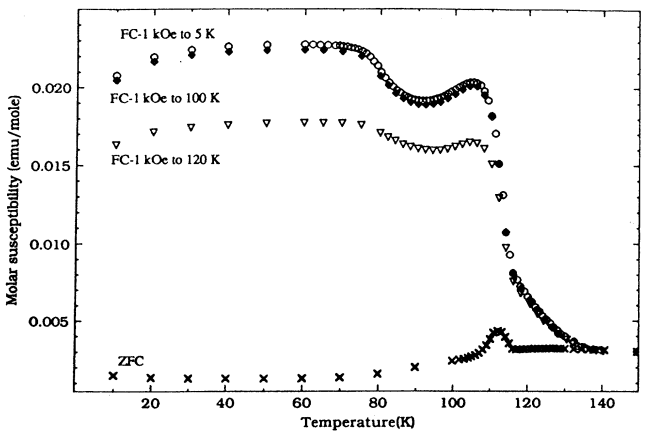

FIG. 7. Molar susceptibility vs temperature curves of YVO_3 taken on heating from 5 K in 1 kOe after the sample is FC ($T > T_a$) for $T_a = 120$, 100, or 5 K.

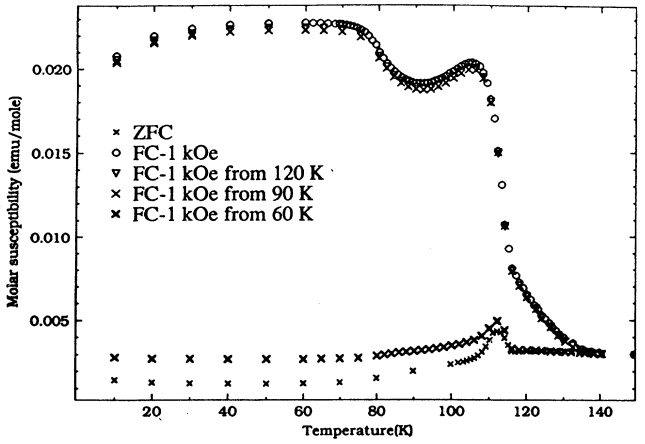

FIG. 8. Molar susceptibility vs temperature curves of YVO_3 taken on heating from 5 K in 1 kOe after sample is ZFC or FC ($T < T_a$) for $T_a = 120$, 90, or 60 K.

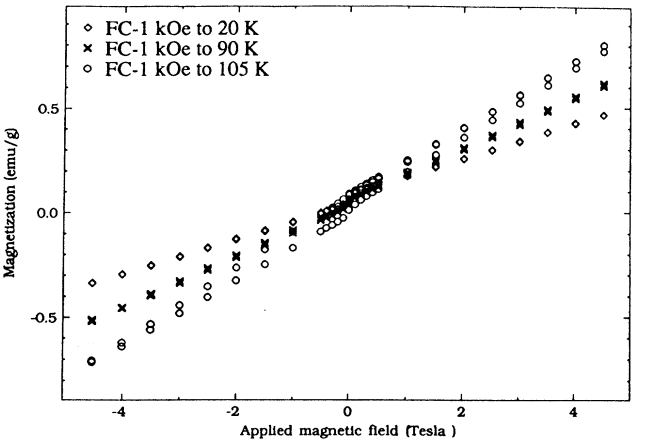

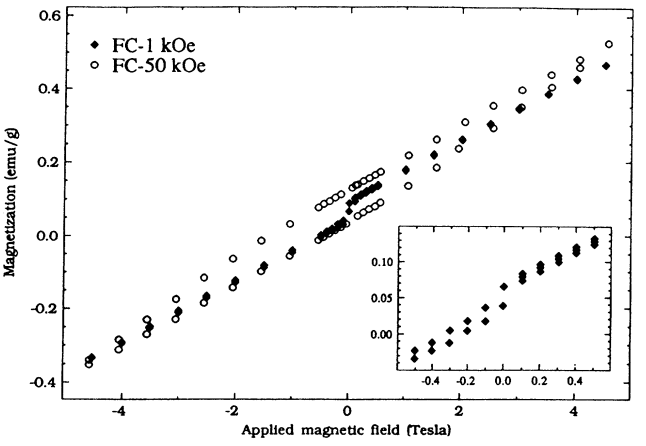

FIG. 9. **M**(**H**) curves for YVO_3 (a) taken at $T_a = 20$, 90, or 105 K after a FC at 1 kOe to T_a, (b) taken at 20 K after a FC at 1 kOe and FC at 50 kOe.

change significantly in 1 kOe the random domain structure established by a ZFC to $T_a < T_s$. However, the $\chi_m(T)$ curve for $T_a = 90$ or 120 K was similar to that obtained after a FC at 1 kOe to 5 K. This experiment shows that the domain configuration established by a ZFC to the interval $T_s < T_a < T_N$ is able to be changed to that established by a FC at 1 kOe through T_N as long as 1 kOe is applied on traversing the spin-configuration change at T_s. In view of a common ferromagnetic axis in the two spin configurations C_yF_x and G_xF_z, this result is not particularly remarkable.

Figure 9(a) shows **M**(**H**) curves for FC 1-kOe samples to 105, 90, or 20 K and measured at the same temperature. These curves show a small hysteresis, a significant displacement to positive magnetization relative to the **M**(**H**) curve obtained after a ZFC, a small reversible change $\Delta\mathbf{M}$ in the magnetization on reversing the sign of **H**, and a lack of saturation of **M** in **H** = 50 kOe. The opening of the hysteresis loop and the susceptibility both increase as T approaches T_N from below. The lack of saturation of **M** reflects primarily the canted-spin character of the ferromagnetism; it does not require a magnetostrictive distortion. The opening of the hysteresis loop of YVO_3 below T_s, Fig. 9(b), is similar to what is found in $LaFeO_3$ where the spin-orbit coupling enters only in second-order perturbation theory. We conclude that the first-order transition at T_s reflects an exchange striction rather than a magnetostriction.

Samples of YVO_3 that were prepared under 15 kbar pressure show similar behavior; there is no evidence for retention of a metastable high-pressure phase such as was found for $LaVO_3$.

F. Magnetization data for $LuVO_3$

Zubkov, Basuev, and Shveikin[11] have reported a G_ZF_x ordered spin configuration below $T_N \approx 101$ K for $LuVO_3$ and $b/\sqrt{2}a > 1$ that decreases linearly with temperature through T_N to liquid-nitrogen temperature. A vanadium moment $\mu_v \approx 1.2\mu_B$ at 4.2 K was also reported. Borukhovich, Zubkov, and Bazuev[19] reported specific-heat anomalies at 97 and 85 K, which they assumed represent T_N and a Jahn-Teller transition temperature T_t, respectively. The specific-heat anomaly at T_N was significantly smaller than that at T_t, which had twin peaks: one at 84 K and the other at 85 K. Moreover, the crystallographic data of Zubkov, Bazuev, and Shveikin[11] showed a smooth variation of lattice parameters down to liquid-N_2 temperature, which would indicate that the transition at 84±1 K is not a Jahn-Teller magnetostrictive distortion; it might be a spin-reorientation within the same G-type magnetic order.

Figure 10 shows $\chi_m(T)$ data taken on heating in 1 kOe after a ZFC and FC at 1 kOe. The two transitions at 83 K and $T_N \approx 105$ K in our sample are both evident. The $\chi_m(T)$ curve for the FC 1-kOe case exhibits a slightly increased susceptibility at 83 K and an abrupt drop in magnetization on heating through T_N. Such an abrupt drop

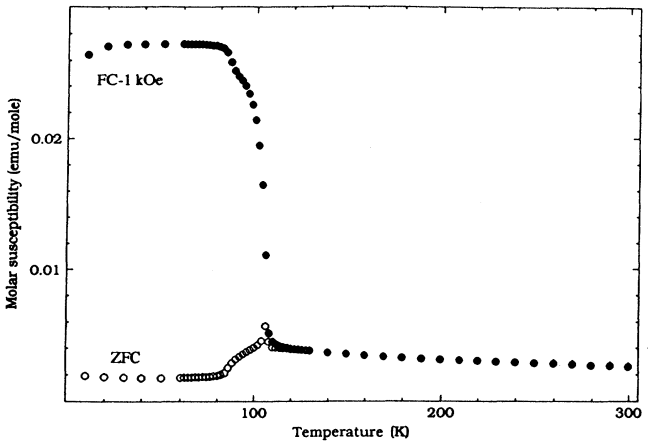

FIG. 10. Molar susceptibility vs temperature curves of $LuVO_3$ measured in 1 kOe after (a) ZFC and (b) FC at 1 kOe from room temperature to 5 K.

is characteristic of a magnetostrictive distortion associated with the magnetic order; however, the Russian data showed a smooth variation of the lattice parameters through T_N.

With a FC ($T > T_a$) at 1 kOe to $T_a = 90$ K and a ZFC from 90 K, the $\chi_m(T)$ curve measured in 1 kOe on heating is similar to that for a FC at 1 kOe to 5 K, whereas a ZFC to $T_a = 90$ K followed by a FC ($T < T_a$) at 1 kOe from 90 to 5 K gives a $\chi_m(T)$ curve on heating similar to the ZFC curve of Fig. 10. Similarly, a FC ($T > T_a$) at 1 kOe to $T_a = 110$ K followed by a ZFC from 110 to 5 K gives a $\chi_m(T)$ curve on heating similar to the ZFC curve.

At 20 K, the **M**(**H**) curves show only a small opening of the hysteresis loop on cycling to 50 kOe; saturation of **M** is not achieved. The FC curve is shifted to $\Delta M > 0$; see Fig. 11.

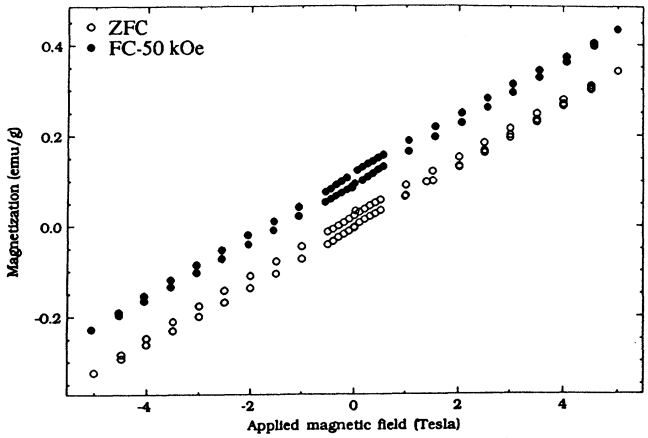

FIG. 11. **M**(**H**) curves of $LuVO_3$ taken at 20 K after a ZFC and FC at 50 kOe.

IV. DISCUSSION

The development of a magnetization oriented antiparallel to the magnetizing field is not entirely without precedent. Menyuk, Dwight, and Wickham[20] have shown such a phenomenon in the ferrimagnetic spinel $Co[CoV]O_4$ if cooled in a magnetic field through a compensation temperature $T_{comp}=70$ K. In this ferrimagnet, the tetrahedral and octahedral Co^{2+} ions with a high-spin configuration couple antiferromagnetically below $T_c=158$ K, and the net magnetization $\mathbf{M}=\mathbf{M}_t-\mathbf{M}_0$ is the difference between the tetrahedral-site and octahedral-site magnetizations $\mathbf{M}_t$ and $\mathbf{M}_0$, each of which vary differently with temperature. Below T_c, the octahedral-site Co^{2+} ions induce a cooperative magnetostrictive distortion (a Jahn-Teller distortion that enhances the orbital angular momentum not quenched by the cubic component of the crystalline field) that creates a giant magnetocrystalline anisotropy. In this case, $\mathbf{M}$ reverses sign at T_{comp} where the ratio $M_t/M_0=1$ occurs, but the giant magnetocrystalline anisotropy does not permit a reorientation of M_t and M_0 on crossing T_{comp}, and so cooling in a magnetic field leaves $\mathbf{M}$ oriented antiparallel to $\mathbf{H}$ below T_{comp}.

Unlike $Co[CoV]O_4$, $LaVO_3$ does not contain two inequivalent magnetic arrays that couple antiparallel to one another to give a T_{comp} where the ZFC $\chi_m(T)$ goes to zero; Fig. 2. Rather, $LaVO_3$ prepared at atomspheric pressure is a canted-spin antiferromagnet having a ferromagnetic component; if it is cooled in a magnetic field $\mathbf{H}$ through a magnetostrictive-distortion onset temperature T_t located only about 4 K below $T_N\approx 142$ K, the net magnetization of a polycrystalline sample is oriented antiparallel to $\mathbf{H}$, giving rise to an anomalous diamagnetism. Moreover, this remarkable phenomenon is not found if the $LaVO_3$ sample is prepared under a hydrostatic pressure $P>8$ kbar; there is no evidence of a weak ferromagnetism in the metastable high-pressure phase, which reverts back to the stable low-pressure phase at 250 °C, even though the Néel temperature of the two perovskite forms of $LaVO_3$ are nearly the same.

The smaller $L=$Y or Lu atoms introduce a larger mismatch between the equilibrium V-O and L-O bond lengths appropriate to the ideal cubic-perovskite structure as defined by Eq. (1), and so the V-O bonds are under a greater compressive stress and the V-O-V bond angle deviates more from 180° on going from La to Y to Lu. A two-phase region in the $La_{1-x}Y_xVO_3$ system and the failure to observe a metastable high-pressure YVO_3 phase indicates that the V-O bonding in YVO_3 is more like that of metastable high-pressure $LaVO_3$ than of stable low-pressure $LaVO_3$. Both YVO_3 and $LuVO_3$ are canted-spin ferromagnets like $LaVO_3$, but neither exhibits the anomalous diamagnetism of $LaVO_3$ if FC at 1 kOe from room temperature to 5 K.

These findings raise the question, what distinguishes $LaVO_3$ from YVO_3, $LuVO_3$, or metastable high-pressure $LaVO_3$? At least four distinguishing features can be identified.

(1) At room temperature, $LaVO_3$ has the O'-orthorhombic structure, whereas all the others are O orthorhombic, and only $LaVO_3$ has been observed to exhibit an abrupt decrease in the ratio $c/\sqrt{2}a$ on cooling below a magnetostrictive distortion $T_t<T_N$.

(2) The antiferromagnetic component of the magnetic order below a T_N is type C in $LaVO_3$, it is type G in the case of low-temperature YVO_3 and $LuVO_3$, and it is without a ferromagnetic component in high-pressure $LaVO_3$. However, YVO_3, like $LaVO_3$, has type-C magnetic order in the interval $T_s<T<T_N$.

(3) In $LaVO_3$, the $T_N-T_t\approx 4$ K temperature difference is small; in YVO_3 and $LuVO_3$ a larger $T_N-T_S>10$ K is indicated. Moreover, in YVO_3 the first-order transition at T_s reduces the volume of the low-temperature phase without any significant change in the magnitude of μ_V.

(4) The V-O bond length is longer and the V-O-V bond angle deviates less from 180° in $LaVO_3$ than in YVO_3, $LuVO_3$, or high-pressure $LaVO_3$.

A room-temperature $c/\sqrt{2}a\leq 1$ in $LaVO_3$ is probably less significant than the observation[9,11] of an abrupt decrease in this ratio on cooling through T_t. A deformation of the individual VO_6 octahedra to a shape having a strong rhombohedral ($\alpha>60°$) component below T_t, Fig. 1(b), is now clearly established.[9] Such a cooperative deformation is predicted below a magnetic-ordering temperature for the case of localized-electron magnetism.[4] However, itinerant electrons do not induce the same type of cooperative Jahn-Teller distortions as localized electrons.[21] Since C-type magnetic order is found for $T_s<T<T_N$ in YVO_3, the lack of any anomaly in the temperature variation of $c/\sqrt{2}a$ down to liquid-nitrogen temperatures appears to be more significant than any difference in the type of magnetic order. The absence of a cooperative magnetostrictive distortion immediately below T_N means that stabilization of the maximum orbital angular momentum in the magnetic configuration at a V^{3+} ion has been suppressed in YVO_3, $LuVO_3$, and high-pressure $LaVO_3$. Such a suppression could be the result of a transition from localized-electron to itinerant-electron antiferromagnetism. In support of this possibility, we note that $CaVO_3$ and $SrVO_3$ are Pauli paramagnetic metals that become itinerant-electron antiferromagnets with a small loss of oxygen.[22–24]

Stabilization of a metastable high-pressure $LaVO_3$ is anomalous; it indicates the presence of a double-well potential for the V-O bond length. This indication is reinforced by the large miscibility gap in the $La_{1-x}Y_xVO_3$ perovskite system. The shorter of the two equilibrium V-O bond lengths is the more stable under pressure. From the absence of a metastable high-pressure phase in YVO_3, we conclude that the bond-length mismatch in YVO_3 and $LuVO_3$ places the V-O bonds under a compressive stress that stabilizes the shorter of the two equilibrium V-O bond lengths.

A similar double-well potential is found in $NdNiO_3$, which exhibits a first-order semiconductor-metal transition at its Néel temperature.[25] The low-temperature phase has the larger volume and the more localized $3d$ electrons; stronger covalent mixing of Ni $3d$ and O $2p$ wave functions in the high-temperature phase delocalizes

the σ-antibonding Ni $3d$ electrons. That we should expect such a transition in a single-valent compound has been argued for some years on the basis of the Virial theorem;[26] it recently has been demonstrated more rigorously.[27] Therefore we interpret the data for the LVO_3 compounds to indicate a first-order transition from localized-electron to itinerant-electron antiferromagnetism on going from $LaVO_3$ to YVO_3 or high-pressure $LaVO_3$. Although the orbital angular momentum remains unquenched in the itinerant-electron regime, it is not enhanced below T_N by a cooperative Jahn-Teller distortion. A volume change $\Delta V<0$ on cooling through T_s in YVO_3 is not obviously compatible with a greater localization of the $3d$ wave function below T_s; it would seem to signal an exchange striction resulting from stronger V-O-V interactions.

The anomalous diamagnetism found for FC 1-kOe $LaVO_3$ is associated with the stabilization of a maximum orbital component of the localized V^{3+}: $3d^2$ configuration below a magnetostrictive Jahn-Teller distortion. Orientation of a magnetization in opposition to a magnetizing field **H** only occurs where a change in field strength induces persistent currents. $LaVO_3$ is an antiferromagnetic insulator; it is not a superconductor. Therefore the only persistent currents that can be influenced by a change in magnetic field are those associated with electrons in stationary electronic states of the atoms. The core electrons have no spin and contribute a weak diamagnetism due to the induced motion of the core electrons. In $LaVO_3$, the anomalously large diamagnetism cannot be attributed to core electrons; it can only be associated with the unquenched orbital angular momentum of the V^{3+}: $3d^2$ configuration, which is maximized below T_t by the magnetorestrictive Jahn-Teller distortion. But the V^{3+}: $3d^2$ configuration also carries a net spin $S=1$, which normally orients its associated moment in the direction of **H** with spin-orbit coupling giving a μ_V that has its orientation determined by the alignment of the spin by **H**. The **M**(**H**) curves of Fig. 11 and Fig. 4 of Ref. 8 show this to be the case in all the LVO_3 perovskites. Moreover, on cooling through T_N, the Dzialoshinskii vector $\mathbf{D}_{ij}$ of the antisymmetric component $\mathbf{D}_{ij}\cdot\mathbf{S}_i\times\mathbf{S}_j$ of the interatomic superexchange interaction has a direction that cants the spins so as to align their ferromagnetic component in the direction of an applied field **H**. It is only on cooling through a magnetostrictive distortion, which enhances the orbital component of μ_V, that the direction of the ferromagnetic component changes sign. The individual μ_V's respond normally to **H** at any given temperature, but an abnormal response may occur where a change ΔV across T_t introduces a ΔL in the magnitude of the orbital angular momentum quantum number and hence of μ_V. We are left to ask whether the observed reversal in the spin of the ferromagnetic component of $LaVO_3$ on cooling or heating through T_t in an applied field **H** is due to a reversal in the sign of μ_V or in the sign of $\mathbf{D}_{ij}$. Since a reversal in the sign of $\mathbf{D}_{ij}$ is equivalent to a reversal in the sign of μ_V, and since rotation of the μ_V is inhibited by a strong magnetocrystalline anisotropy, we are led to consider the possibility of reversal in the sign of μ_V on traversing T_t.

To address this possibility, we note that a first-order change in the magnitude of μ_V at a V^{3+} ion on traversing a first-order magnetostrictive phase-transition temperature T_t would induce a persistent atomic current that opposes the change and therefore a reversal of the sign of the orbital quantum number **L**. Spin-orbit coupling would then invert the sign of μ_V since the spin-orbit coupling is stronger than the Zeemann coupling of the spin to **H**.

The shorter equilibrium V-O bond length in YVO_3, $LuVO_3$, and high-pressure $LaVO_3$ increases the V-O covalent mixing. A large deviation of the V-O-V bond angle from 180° may retain strongly correlation V^{3+}:d^2 configurations, but the enhanced covalent mixing suppresses the cooperative Jahn-Teller distortion normally associated with localized octahedral-site $3d^2$ configurations. In the absence of a first-order magnetostrictive distortion below T_N across which the orbital angular momentum is discontinuously changed, no anomalous diamagnetism is observed.

V. CONCLUSION

The anomalous diamagnetism that has been reported for $LaVO_3$ cooled in a magnetic field of 1 kOe has been shown to be due to a reversal of the ferromagnetic component of a canted-spin antiferromagnet on cooling through a cooperative, first-order magnetostrictive distortion setting in at a $T_t<T_N$. This reversal of the ferromagnetic component of the canted-spin configuration is not found in YVO_3, $LuVO_3$, or a metastable high-pressure $LaVO_3$ having the same structure; in none of these perovskites do we find a magnetostrictive distortion setting in at $T_t<T_N$.

On cooling or heating across the transition temperature T_t in $LaVO_3$, there is a first-order change in the orbital angular momentum of the ${}^3T_{1g}$ configuration at an octahedral-site V^{3+}: $3d^2$ ion. We propose that the resulting change $d\mu_V/dt$ on crossing T_t induces a persistent atomic current that opposes the magnetic field associated with $\Delta\mu_V$, thereby reversing the sign of **L** and hence the direction of μ_V. In an applied magnetic field that orients the ferromagnetic component preferentially in the direction of **H** on cooling through T_N, a reversal in the direction of the μ_V is manifest as a reversal in the direction of the sample magnetization **M**. In the absence of a net magnetization **M** in a sample cooled in zero field, the value of χ_m is independent of the direction of the individual atomic moments μ_V in zero field and a reversal of the directions of the μ_V would not be detected in a χ_m curve.

Suppression of the first-order magnetostrictive distortion at a $T_t<T_N$ in high-pressure $LaVO_3$ is attributed to stabilization of a shorter equilibrium V-O bond length in which a greater covalent mixing delocalizes the antibonding $3d$ electron at a V^{3+} ion out over the nearest-neighbor ligands. This delocalization suppresses the cooperative Jahn-Teller distortion even though bending of the V-O-V bond from 180° retains a narrow π^* band

and a localized atomic moment μ_V; bending of the V-O-V bond angle reduces the overlap integral of the t_2 orbital on neighboring V^{3+} ions while shortening the V-O bond length enhances the V-O covalent bonding.

The observation of a different equilibrium V-O bond length in high-pressure $LaVO_3$ manifests itself as a large two-phase compositional range in the system $LaVO_3$-YVO_3. This two-phase range and the absence of a high-pressure phase in YVO_3 indicates that YVO_3 exerts sufficient chemical pressure on the V-O bond to stabilize the shorter equilibrium V-O bond length. A similar situation applies to $LuVO_3$. The transition to a shorter equilibrium V-O bond length is also a manifestation of the fact that V^{3+} in an octahedral site is close to the metal-insulator transition for V-O-V bonding. The perovskites $CaVO_3$ and $SrVO_3$ contain itinerant electrons; the stronger covalent bonding with V^{4+} ions transforms the localized V-t_2 electrons into narrow π^* band electrons.

ACKNOWLEDGMENTS

We thank the Robert A. Welch Foundation, Houston, Texas, and the National Science Foundation for financial support.

[1]J. B. Goodenough and J. M. Longo, in *Crystallographic and Magnetic Properties of Perovskite and Related Compounds,* edited by K. H. Hellwege, Landolt-Bornstein, New Series, Group X, III/4a, Pt. x (Springer-Verlag, Berlin, 1970), p. 126.

[2]B. K. Vainshtein, V. M. Fridkin, and V. L. Indenbom, *Modern Crystallography II, Structure of Crystals,* Vol. 21 of Solid-State Science (Springer-Verlag, Berlin, 1982), Chap. 1, Table 1.8a.

[3]J. Kanamori, Prog. Theor. Phys. (Kyoto) **17**, 177 (1957); **17**, 197 (1957).

[4]J. B. Goodenough, Phys. Rev. **171**, 466 (1968).

[5]H. C. Nguyen and J. B. Goodenough (unpublished research).

[6]N. Shirakawa and M. Ishikawa, Jpn. J. Appl. Phys. **30**, L 755 (1991).

[7]A. V. Mahajan, D. C. Johnston, D. R. Torgeson, and F. Borsa, Physica C **185-189**, 1095 (1991); Phys. Rev. B **46**, 10966 (1992).

[8]J. B. Goodenough and H. C. Nguyen, C. R. Acad. Sci. **319**, 1285 (1994).

[9]P. Bordet, C. Chaillout, M. Marezio, Q. Huang, A. Santoro, S.-W. Cheong, H. Takagi, C. S. Oglesby, and B. Batlogg, J. Solid State Chem. **106**, 253 (1993).

[10]Q. Huang, A. Santoro, P. Bordet, M. Marezio, S.-W. Cheong, and B. Batlogg (private communication).

[11]V. G. Zubkov, G. V. Bazuev, and G. P. Shveikin, Sov. Phys. Solid State **18**, 1165 (1976).

[12]P. Dougier and P. Hagenmuller, J. Solid State Chem. **11**, 177 (1977).

[13]A. S. Borukhovich, G. V. Bazuev, and G. P. Shveikin, Sov. Phys. Solid State **16**, 181 (1974); **15**, 1467 (1974).

[14]A. S. Borukhovich and G. V. Bazeuv, Sov. Phys. Solid State **16**, 181 (1978).

[15]H. Kawano, H. Yoshizawa, and Y. Ueda, J. Phys. Soc. Jpn. **63**, 2857 (1994).

[16]E. F. Bertaut, in *Magnetism: A Treatise on Modern Theory and Materials,* edited by G. T. Rado and H. Suhl (Academic, New York, 1963), Chap. 4.

[17]W. C. Koehler, E. O. Wollan, and M. K. Wilkinson, Phys. Rev. **118**, 58 (1960).

[18]A. S. Borukhovich, G. V. Bazuev, and G. P. Shveikin, Sov. Phys. Solid State **16**, 191 (1974).

[19]A. S. Borukhovich, V. G. Zubkov, and G. V. Bazuev, Sov. Phys. Solid State **20**, 1049 (1978).

[20]N. Menyuk, K. Dwight, and D. G. Wickham, Phys. Rev. Lett. **4**, 119 (1960).

[21]J. B. Goodenough, Prog. Solid State Chem. **5**, 145 (1971).

[22]J. B. Goodenough, J. A. Kafalas, and J. M. Longo, in *Preparative Methods in Solid State Chemistry,* edited by P. Hagenmuller (Academic, New York, 1972), Chap. 1.

[23]A. Fukushima, K. Iga, I. H. Inoue, K. Murata, and Y. Nishihara, J. Phys. Soc. Jpn. **63**, 409 (1994); F. Iga and Y. Nishiara, *ibid.* **61**, 1867 (1992).

[24]P. Dougier, J. C. C. Fan, and J. B. Goodenough, J. Solid State Chem. **14**, 247 (1975).

[25]J. B. Torrance, P. Lacorre, A. I. Nagzal, E. J. Ansaldo, and Ch. Neidermayer, Phys. Rev. B **45**, 8209 (1992).

[26]P. Majumdar and H. R. Krishnamurthy, Phys. Rev. Lett. **73**, 1525 (1994).

[27]T. Moriya, in *Magnetism: A Treatise on Modern Theory and Material,* edited by G. T. Rado and H. Suhl (Academic, New York, 1963), Vol. 1.